Decentralized Method for Load Sharing and Power Management in a Hybrid Single/Three-Phase-Islanded Microgrid Consisting of Hybrid Source PV/Battery Units

Karimi, Yaser; Oraee, Hashem; Guerrero, Josep M.

Published in:
I E E E Transactions on Power Electronics

DOI (link to publication from Publisher):
10.1109/TPEL.2016.2620258

Publication date:
2017

Document Version
Early version, also known as pre-print

Decentralized Method for Load Sharing and Power Management in a Hybrid Single/Three-Phase Islanded Microgrid Consisting of Hybrid Source PV/Battery Units

Yaser Karimi, Hashem Oraee, *Senior Member, IEEE,* Josep M. Guerrero, *Fellow, IEEE*

***Abstract*— This paper proposes a new decentralized power management and load sharing method for a photovoltaic based, hybrid single/three-phase islanded microgrid consisting of various PV units, battery units and hybrid PV/battery units. The proposed method is not limited to the systems with separate PV and battery units, and power flow among different phases is performed automatically through three-phase units. The proposed method takes into account the available PV power and battery conditions of the units to share the load among them. To cover all possible conditions of the microgrid, the operation of each unit is divided into five states in single-phase units and seven states in three-phase units and modified active power-frequency droop functions are used according to operating states. The frequency level is used as trigger for switching between the states. Efficacy of the proposed method in different load, PV generation and battery conditions is validated experimentally in a microgrid lab prototype consisted of one three-phase unit and two single-phase units.**

***Index Terms*— decentralized power management; hybrid single/three-phase microgrid; hybrid source microgrid; hybrid PV/battery unit; SoC; PV power curtailment;**

I. Introduction

Microgrids (MGs), that can be considered as local grids consisting of distributed generators (DGs), energy storage systems and loads, are becoming more attractive due to high penetration of DGs, specially photovoltaic (PV) generations [1-5]. Depending on load and generation requirements, the MG system can be in one of single-phase, three-phase or hybrid single/three-phase configurations. In a hybrid single/three-phase MG, as shown in Fig. 1, single-phase loads, PV and battery units are connected to different phases of a three-phase MG. When the grid is present, the circuit breaker (CB) is closed and the MG operates in grid-connected mode to exchange power with the main utility, and the battery storage can perform different roles such as frequency control, instantaneous reserve, and peak shaving [6, 7] . If a disturbance occurs in the main utility, the MG is disconnected to operate in islanded mode [8]. Battery storage can be connected as a separate unit to the MG or can be combined with the PV unit forming a hybrid source unit [7, 9, 10]. While both configurations are widely used, the latter is more cost effective because of higher efficiency and lower component cost.

In islanded mode of operation, the control system objectives are sharing the load among different units and balancing the power in the MG while considering power rating and PV generation of the units and State of Charge (SoC) of the batteries [11, 12]. These objectives can be achieved by centralized [13-18] or decentralized [9, 19-26] power management. The centralized control strategies rely on communication among units and loads in the MG, which reduces the reliability of the system [22, 27]. The decentralized control methods, however, only require local measurements. In addition, non-crucial communication can be used along with the decentralized control to achieve other objectives such as restoring voltage and frequency deviations [28, 29]. Several decentralized control strategies for power management of islanded MGs consisting of DGs and batteries have been proposed in the literature. In [19-21] frequency signaling technique is utilized for the power management. However, the applications of these methods are limited to the MGs composed of only one energy storage unit. In [25] a SoC balancing scheme for microgrids with distributed separate battery storage units is proposed which adds a SoC-based droop control to the conventional droop control. In [22] a frequency based energy management strategy is proposed for a MG with distributed battery storage but it is only valid for systems with separate battery units. Similarly, the frequency bus-signaling method proposed in [23] is only applicable to separate battery units. In [24], separate battery storage and PV units are controlled based on modified droop method, whereas in [9] the method is adapted for a single PV/battery hybrid unit connected to a droop controlled MG. However, those methods are not applicable to the MGs consisting of multiple hybrid units. In [30] a power management and load sharing strategy is proposed by the authors which overcomes these drawbacks.

All the aforementioned references present power management strategies for single-phase or three-phase MGs. However, in a hybrid single/three-phase MG, the power management is more challenging because control of the power flow among different phases is necessary in this configuration. For the best knowledge of the authors, only [31] deals with this issue. In this reference, a power sharing unit (PSU) composed of three single-phase back-to-back converters connected between the phases is used to control the power flow among them. The disadvantage of this method is the necessity of installing the PSU which makes it not applicable to existing structures. In addition, it requires the real-time values of total generated power and load power of each phase to determine the PSU mode.

Manuscript received April 18, 2016; revised July 22 and September 8, 2016; accepted October 6, 2016.

Y. Karimi and H. Oraee are with the Department of Electrical Engineering, Sharif University of Technology, Tehran, Iran, 11365-11155 (emails: y_karimi@ee.sharif.edu, oraee@sharif.edu).

J. M. Guerrero is with the Department of Energy Technology, Aalborg University, 9220 Aalborg East, Denmark (e-mail: joz@et.aau.dk).

Color versions of one or more of the figures in this paper are available online at http://ieeexplore.ieee.org.

Digital Object Identifier 10.1109/TPEL. 2016-04-0727

This paper proposes a decentralized method for power management and load sharing in an islanded hybrid single/three-phase MG consisting of different single-phase or three-phase PV units, battery storage units and hybrid PV/battery units. To achieve the decentralized power management, conventional active power-frequency (*P-f*) droop equation [1, 8, 32, 33] is modified according to each operating state of the units; moreover, the frequency level is used to trigger state changes in each unit. The proposed method has the following features and the contribution of the paper is providing them without relying on any communications or central management system.

- It provides power management for hybrid single/three-phase MGs consisting of PV, battery and hybrid PV/battery SPUs and TPUs.
- When the total load of the MG is more than total PV generation, all PV sources (in both separate and hybrid units, in both SPUs and TPUs) operate in Maximum Power Point (MPP) and all the batteries contribute in supplying the surplus load power. Furthermore, the surplus power is shared among the batteries so that batteries with higher SoC have higher discharging power.
- In case that the total PV generation is more than total load and the batteries in the MG have the capacity to absorb the surplus power, the batteries are charged with the excess PV power. The excess power is shared among the batteries so that batteries with lower SoC absorb more power.
- When the total PV generation is more than total load and all batteries are completely charged or reach their maximum charging power, PV power curtailment is performed.
- Power flow among different phases is performed automatically through TPUs, so that loads on a phase can be supplied from the generation in other phases, or batteries can be charged from the excess power of other phases.

The rest of the paper is organized as follows: in section II, the general structure of the hybrid source hybrid single/three-phase MG is presented. In section III, the proposed method is presented in detail. The proposed method is validated experimentally in section IV. Section V concludes the paper.

II. Hybrid Source, Hybrid Single/Three-Phase Microgrid Structure

A hybrid single/three-phase MG consisting of SPUs, TPUs, single-phase and three-phase loads is depicted in Fig. 1. The grid is connected through a Δ-Y transformer and a circuit breaker to the three-phase four-wire MG. Only the islanded operation of the MG is studied in this paper and the CB is considered open. The source of the units can be PV, battery or hybrid PV/battery. In order to simplify presenting the results, the MG shown in Fig. 2 is considered in this paper. It consists of a PV sourced TPU and two hybrid sourced SPUs connected to phases-a and b, named SPU-a and SPU-b, respectively. There is no SPU connected to phase-c. All the MG loads are centralized in three single-phase loads connected to the three phases of the MG. The SPUs consist of a half-bridge inverter connected to the Point of Common Coupling (PCC) through a LCL filter, a PV array connected to the dc-link via a dc-dc boost converter and a battery storage connected to the dc-link via a bidirectional dc-dc boost converter. The TPU consists of a three-phase four-wire

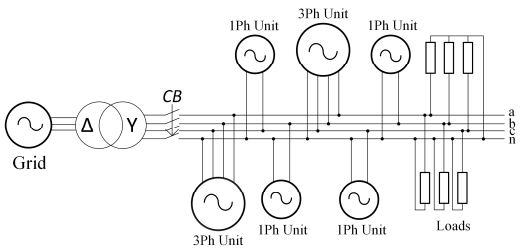

Fig. 1 Typical hybrid single/three-phase microgrid

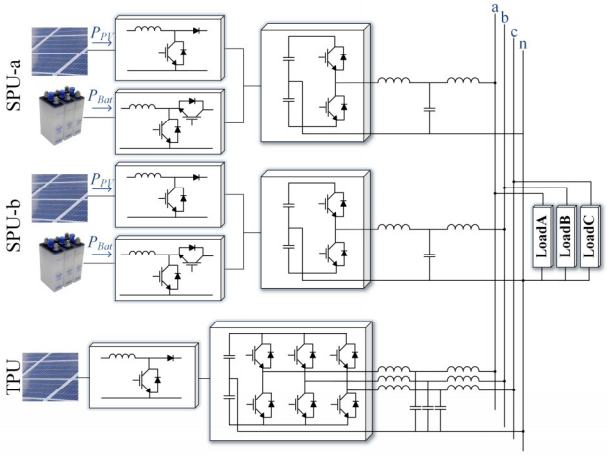

Fig. 2 Hybrid source, hybrid single/three-phase islanded microgrid structure studied in the paper

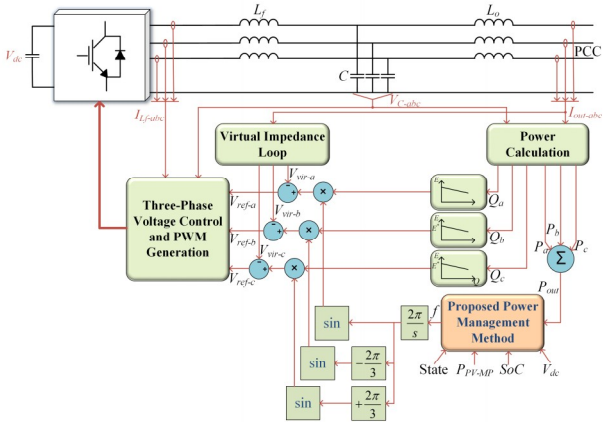

Fig. 3 Control structure of the inverter part of each TPU

inverter connected to the PCC through a LCL filter and a PV array connected to the dc-link via a dc-dc boost converter.

By using an inductance in the output filter of each unit and by implementing virtual inductance [34, 35], it is ensured that the output impedance of units is mainly inductive. Therefore, the modified *P-f* droop functions which will be described in the next section along with the conventional *Q-E* droop can be applied for active and reactive power sharing, respectively.

The control structure of the inverter part of TPUs has been shown in Fig. 3. The control structure of SPUs is same as [30]. Control of the dc-dc converters are well described in [9, 21] and are not addressed in this paper. The inverter control system of both SPUs and TPUs compose of five main parts: Power Calculation, output voltage amplitude calculation, output voltage frequency calculation, Virtual Impedance Loop, and Voltage Control Loop and PWM Generation. Since this paper only focuses on active power management and reactive power control is out of scope of this paper, the

amplitude of output voltage reference is determined by the conventional droop equation.

The frequency of the output voltage reference, in both SPUs and TPUs, is calculated based on a new frequency signaling method, as detailed in the following section. A virtual impedance (R_v+jL_v) is added using the Virtual Impedance block as described in [36] to decouple the active and reactive power regulations. Proportional-Resonant (PR) controller [32] is used for inner voltage and current control loops to track the reference voltage.

III. Proposed Power Management Method

In this section, the details of the decentralized control strategy for active power management and load sharing in a hybrid source hybrid single/three-phase MG are discussed. Note that this paper is only focused on active power sharing and reactive power sharing is out of scope of the paper. First, the general operating modes of the whole MG are presented; then, the operating states of each hybrid unit and criteria for changing of the states are described.

A. The Microgrid Operating Modes

Depending on the load, maximum available PV power and charging capacity of the batteries, the MG can operate in three main modes. In order to achieve the decentralized power management and load sharing, the following general droop function, which is used for both SPUs and TPUs, is modified according to MG operating mode to determine output voltage frequency, *f*.

$$f = f_0 + (m_p + \frac{m_i}{s})(P_{ref} - P_{out}) \quad (1)$$

where f_0 is the nominal frequency of the MG, P_{out} is the total output power of the unit, m_p, m_i and P_{ref}, that are determined according to operating mode and are passed through a Low-Pass Filter (LPF) for smooth state transition, are proportional and integral droop coefficients and power reference value, respectively.

Mode I)

In this mode, the total MG load is larger than total PV maximum power and the batteries in the MG supply the surplus load power. Units can be in States 1, 4, 5 or 5a as detailed in the next section.

In this mode, the PV boost converter in all units perform maximum power point tracking, for example by Perturb & Observe algorithm, and try to inject the maximum power to dc-link. Load is shared among the units such that the total discharging power of the batteries is shared among the units based on the SoC and capacity of the corresponding battery. The *P-f* droop function parameters in this mode are as follows, in which, to achieve SoC balancing, the droop coefficient is adaptively updated based on the SoC, similar to method proposed in [37, 38] for DC MGs. In addition, P_{ref} is chosen equal to $P_{PV\text{-}MP}$ of the unit to allow the PV to work in MPP. Note that, $P_{PV\text{-}MP}$ is the instantaneous measured value of the PV power which is injected to the dc-link by PV boost converter. This power is expected to be the PV maximum power but may be different from the actual PV maximum power based on the MPPT algorithm.

$$m_p = m_{pd0}\frac{1}{SoC^n}\ ,\ m_i = 0\ ,\ P_{ref} = P_{PV-MP} \quad (2)$$

where m_{pd0} is a constant value that is selected such that the system is stable in the possible range of SoC and is inverse proportional to battery capacity, and n adjusts the SoC balancing speed [37, 38]. Neglecting the converter power losses, the discharging power of the battery is expressed as follows:

$$P_{Bat} = P_{out} - P_{PV}\ , \quad (3)$$

therefore, (1), using the parameters of (2), is equal to

$$f = f_0 - m_p P_{Bat} \quad (4)$$

which results in distribution of discharging power according to the SoC and battery capacity. It is worth mentioning that P_{Bat} is positive in discharging mode and is negative in charging mode.

Mode II)

In this mode, the MG load is less than total PV maximum power but the batteries have the capability to absorb the surplus PV power. Therefore, all PVs work at MPP and the batteries are charged with the surplus power. Based on SoC and rating of the batteries, some units may be in charge limiting state to limit charging power of the battery (State 2).

For the units which are not in charge limiting state, V_{dc} is regulated by the battery boost converter, the inverter is in Voltage Control Mode (VCM) and the output power is controlled according to the following *P-f* droop function parameters:

$$m_p = m_{pc0}SoC^n\ ,\ m_i = 0\ ,\ P_{ref} = P_{PV-MP} \quad (5)$$

in which droop coefficient is adjusted proportional to SoC of the battery, similar to method proposed in [38] for DC MGs, so that batteries with higher SoC absorb less power.

For the units which are in charge limiting state, the inverter is in Power Control Mode (PCM) and the output power is controlled by the following droop parameters:

$$m_p = K_{PP}, m_i = K_{PI}, P_{ref} = (K_{VP} + \frac{K_{VI}}{s})(V_{dc} - V_{dc}^*) \quad (6)$$

where V_{dc}^* is the reference value of dc-link voltage, K_{VP} and K_{VI} are proportional and integral gains of V_{dc} controller and K_{PP} and K_{PI} are proportional and integral gains of output power controller. In steady-state conditions, neglecting the power losses,

$$P_{ref} = P_{PV-MP} - |P_{ChLimit}|, \quad (7)$$

where $P_{ChLimit}$<0 is the maximum permissible charging power of the battery which depends on the rating, voltage and charging state of the battery and is zero when battery reaches SoC_{max}. This control strategy enables distributing the charging power among the batteries. So, each battery can be charged with PV power of other units.

Mode III)

In this mode, the sum of MG load and total charging capacity of the batteries is less than total PV maximum power. Therefore, in order to keep the power balance, PV power curtailment should be performed in some units. In this mode, all batteries are charged with maximum power, units that have sufficient PV power to provide both battery charging power and output power determined by droop function (8) are controlled in VCM and PV boost converter regulates the dc-link voltage (corresponding to State 3). Other units work at MPP and are controlled in PCM based on (6) (corresponding to State 2). The conventional *P-f* droop is used for VCM units in this mode and the droop parameters are, as follows:

$$m_p = \frac{\Delta f_{max}}{P_{out-max}}\ ,\ m_i = 0\ ,\ P_{ref} = 0 \quad (8)$$

B. Operating States of Each Unit in the Microgrid

In this section, the operating states of a single unit in the MG and criteria for state changes are presented.

Each SPU in the MG can operate in one of the following states: 1. Battery charge-discharge, 2. Battery charge limit, 3. PV power curtailment, 4. Battery disconnect, 5. Output power limit [30].

Each TPU in the MG can be in one of the aforementioned five states or the following states: 5a. Phase output power limit, 5b. Phase output power and battery charge limit

The control strategy in each state and the criteria for transition between the states are detailed in the following:

State 1:

This state corresponds with the normal operation of the unit, i.e., when neither the SoC nor the currents have reached the limits. In this state, the frequency is adjusted according to (2) or (5), depending on the discharging or charging of the battery. In this state, PV works at MPP and battery boost converter regulates V_{dc}.

The unit can exit the state 1 in case one of the following criteria is met:

- The battery is completely charged or the battery power reaches the maximum charging power due to decrease in load or increase in PV generation; In this case, the state is changed to State 2.
- The *SoC* reaches to its minimum value, SoC_{min}. In this case, the state is changed to State 4.
- The output power reaches the inverter rating, $P_{out\text{-}max}$. In this case, the state is changed to State 5.
- Only in TPUs: The output power of one phase reaches its limit value, $P_{phase\text{-}max.}$ In this case, the state is changed to State 5a.

State 2:

This state is regarded as the transition state between States 1 and 3. It is a common state in Modes II and III of the MG operating modes in which the unit operates in PCM. The unit enters this state when battery charge limit occurs in State 1 or the unit reaches PV maximum power in State 3. In this state, PV works at MPP, battery is charged with maximum power and V_{dc} is regulated by (6). With this control, the difference between PV power and battery charging power is injected to/absorbed from the MG. Neglecting power losses, the output power of the unit is determined by (7) in steady-state conditions.

The criteria for exiting from State 2 depend on the previous state of the unit and are as follows:

- All units enter this state one by one from State 1 because of load drop, decrease in battery charging power or PV generation rise. In this case, *f* gradually increases due to the integration action in (6) until it saturates to f_{max}. At this point, all units change to State 3 to reduce PV power generation and maintain the power generation/consumption balance.
- When the MG is in Mode II, in which, all units are in State 2 or charging mode of State 1, any increase in load or decrease in PV generation reduces total charging power of the MG. In this case, the imbalance among charging powers of the units is increased because units in State 2 are controlled in constant power and only charging powers of units in State 1 are decreased. To ensure balanced distribution of charging power (with considering SoC of the batteries), each unit that is in State 2 should exit constant power control mode and return to State 1 when the following criterion is met [30] in which $K_{pm}<1$ is a margin used for preventing unwanted changing of state because of error in power measurement:

$$f < f_0 - K_{pm} m_p P_{Bat} \text{ and preState} = 1. \quad (9)$$

- All units enter this state one by one from State 3 because of increase in load or decrease in PV generation. In this case, *f* gradually decreases due to the integration action in (6) until it saturates to f_{min}. At this point, all units change to State 1 in order to reduce the battery charging power or enter battery discharging mode.
- When the MG is in Mode III in which all units are in State 3 or State 2, any decrease in load or battery charging power reduces the required PV generation in the MG. In this case, since units in State 2 are controlled in MPP, PV generation of units in State 3 are decreased which increases the uneven distribution of output power and PV generation among the units. To overcome this, each unit in State 2 should return to State 3 when the following criterion is met [30]:

$$f > f_0 - K_{pm} m_p P_{out} \text{ and preState} = 3. \quad (10)$$

- Only in TPUs: The output power of one phase reaches its limit value, $P_{phase\text{-}max.}$ In this case, the state is changed to State 5b.

State 3:

This state is associated with Mode III of the MG operating modes in which total PV maximum power is more than total power required by load and charging of the batteries. In this state, the unit's battery is charged with maximum power, output power is controlled by (8) and PV boost converter regulates V_{dc}. In this state, PV power, that is the sum of output power and battery charging power, is less than the MPP.

The criterion for exiting from State 3 is as follows:

- The PV maximum power is less than the sum of output power determined by (8) and battery charging power. In this case, PV boost converter is not able to regulate V_{dc} and it drops below a critical threshold. At this point the unit is switched to State 2. This can occur due to load rise, PV generation drop or in case that all units enter State 3 from State 2 but PV power is not sufficient for this unit.

State 4:

When *SoC* of the battery reaches to SoC_{min}, the unit enters this state. In this state, battery is disconnected to prevent damage due to its deep discharging, PV works at MPP and V_{dc} is regulated by (6). Since P_{Bat}=0, in the steady-state,

$$P_{out} = P_{PV-MP}. \quad (11)$$

The criterion for exiting from State 4 is as follows:

- According to (2) and (5), if $f>f_0$ it indicates that $P_{Bat}<0$ in units that are in State 1, which means, they are in battery charging mode. At this point, this unit can return to State 1 to charge the battery.

State 5:

In both SPUs and TPUs, when output power of the unit reaches $P_{out\text{-}max}$, the unit enters this state to limit its output power. In this state, PV works at MPP and V_{dc} is regulated by the battery boost converter, which controls the battery in discharging mode. The output power is controlled by (6) with $P_{ref}= P_{out\text{-}max}$.

The criterion for exiting from State 5 is as follows:

- The load is decreased such that the weighted battery discharging power (m_pP_{Bat}) of other units in State 1 is less than this unit's corresponding value, i.e.

$$m_{p-i} P_{Bat-S1-i} < K_{pm} m_p P_{Bat}. \quad (12)$$

In this case, the unit can return to State 1. According to (2), this criterion can be written as,

$$f > f_0 - K_{pm} m_p P_{Bat}. \quad (13)$$

When this criterion is met and the unit returns to State 1, the unit will no longer enter State 5.

State 5a and State 5b:

As will be described in the next section, in a TPU, the power of different phases may have different directions. Therefore, the output power of one phase may reach its maximum value while the total output power is less than $P_{out\text{-}max}$. In this case, P_{out} must be reduced to less than $P_{out\text{-}max}$ to ensure that output powers of all phases are in the permissible range. To achieve this, a PI controller is used to limit the output power, as follows:

$$P_{ref} = P_{out\text{-}max} + (K_p + \frac{K_I}{s})(P_{ph\text{-}max} - P_{ph-x}) \quad (14)$$

where $P_{ph\text{-}x}$ and $P_{ph\text{-}max}$ are the output power of the phase that is overloaded and its limit value, respectively.

In State 5a, battery is not in charge limiting mode and can absorb the surplus PV power when output power is reduced less than $P_{PV\text{-}MP}$. In this state, PV works at MPP and battery boost converter regulates V_{dc}.

In State 5b, battery is in charge limiting mode, P_{PV} is reduced less than $P_{PV\text{-}MP}$ and PV boost converter regulates V_{dc}.

The criteria for exiting from State 5a is as follows:

- Same as State 5, if (13) is met, unit can return to State 1.
- If battery reaches charge limiting mode, unit changes to State 5b.

The criterion for exiting from State 5b is as follows:

- If PV power reaches its maximum value, $P_{PV\text{-}MP}$, unit returns to State 2.

Fig. 4 summarizes the criteria for transition between the states. States 5a and 5b do not exist in SPUs.

C. Power flow among different phases

In order to analyze the autonomous power flow among different phases through the TPUs, the MG shown in Fig. 2 is considered. Different cases can happen in the operation of the MG. In the case that all units work in State 3, (8) determines the output powers of the units. Since in steady-state, the frequencies of all units are the same, the following relationships exist between the total and phase output power of TPU and output powers of SPUs,

$$\left.\begin{aligned} f &= f_0 - m_{TPU} P_{TPU} \\ f &= f_0 - m_{SPUa} P_{SPUa} \\ f &= f_0 - m_{SPUb} P_{SPUb} \end{aligned}\right\} \Rightarrow \begin{aligned} m_{TPU} P_{TPU} &= m_{SPUa} P_{SPUa} \\ &= m_{SPUb} P_{SPUb} \end{aligned} \quad (15)$$

$$P_{TPU} = P_{TPUa} + P_{TPUb} + P_{TPUc}$$

In addition, power balance in each phase of the MG results in the following equations,

$$P_{TPUa} + P_{SPUa} = P_{LDa}; \; P_{TPUb} + P_{SPUb} = P_{LDb}; \quad (16)$$
$$P_{TPUc} = P_{LDc}$$

where P_{LDx} is load power of each phase. Using this set of equations, the output powers of SPUs and each phase of the TPU can be determined exactly. Note that P_{TPUa}, P_{TPUb} or P_{TPUc} can be negative which means that power is transferred from one phase to another. In other cases, similar equations determine the output powers. For example, if SPU-a is in State 2 and other units are in State 3, (15) can be written as,

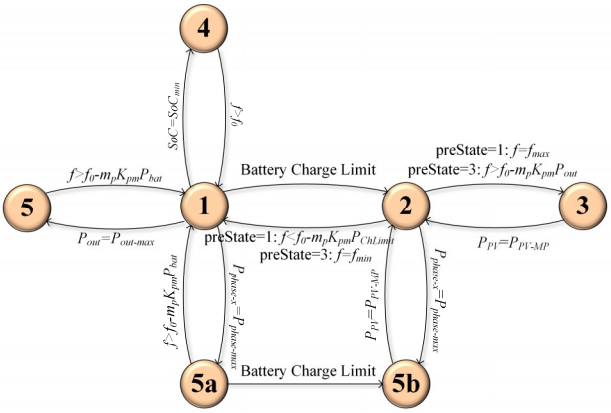

Fig. 4 Criteria for transition between the states in each unit in the MG

Fig. 5 Experimental setup

$$\left.\begin{aligned} f &= f_0 - m_{TPU} P_{TPU} \\ f &= f_0 - m_{SPUb} P_{SPUb} \end{aligned}\right\} \Rightarrow m_{TPU} P_{TPU} = m_{SPUb} P_{SPUb} \quad (17)$$

$$P_{SPUb} = P_{refb}$$

$$P_{TPU} = P_{TPUa} + P_{TPUb} + P_{TPUc}$$

I. Experimental Results

The proposed method has been evaluated experimentally on the MG of Fig. 2 using the setup shown in Fig. 5. It consists of three Danfoss inverters, a real-time dSPACE1006 platform, Inductor-Capacitor-Inductor (LCL) filters and load. Batteries and PVs are modeled in MATLAB and emulated in the dSPACE controller. The experimental setup and controller parameters are listed in Table I.

Several experiments are performed to evaluate the performance of the proposed method in different possible conditions of the MG. In all experiments, K_{pm}=0.8. Since there is no SPU on phase-c, P_{TPUc}=P_{LDc} in all cases. The TPU only works in States 2, 3, 5 and 5b because it has no battery.

Fig. 6 shows the state, load powers of each phase, output powers of TPU and SPUs, output powers of each phase of TPU, PV power, battery power and output frequency when load is decreased and increased step by step and the irradiance is kept constant. For clarity of the results in this experiment, m_p is considered independent of the SoC in the SPUs; moreover, since the rating of the TPU is three times the SPUs, m_p of the TPU in State 3 is one-third of the SPUs. The $P_{PV\text{-}MP}$ of TPU, SPU-a and SPU-b are considered 540W, 255W and 210W, respectively and the $|P_{ChLimit}|$ of the SPU-a and SPU-b are 110W and 250W, respectively. Initially, total load power (1175W) is higher than total $P_{PV\text{-}MP}$ (1005W) and the MG is

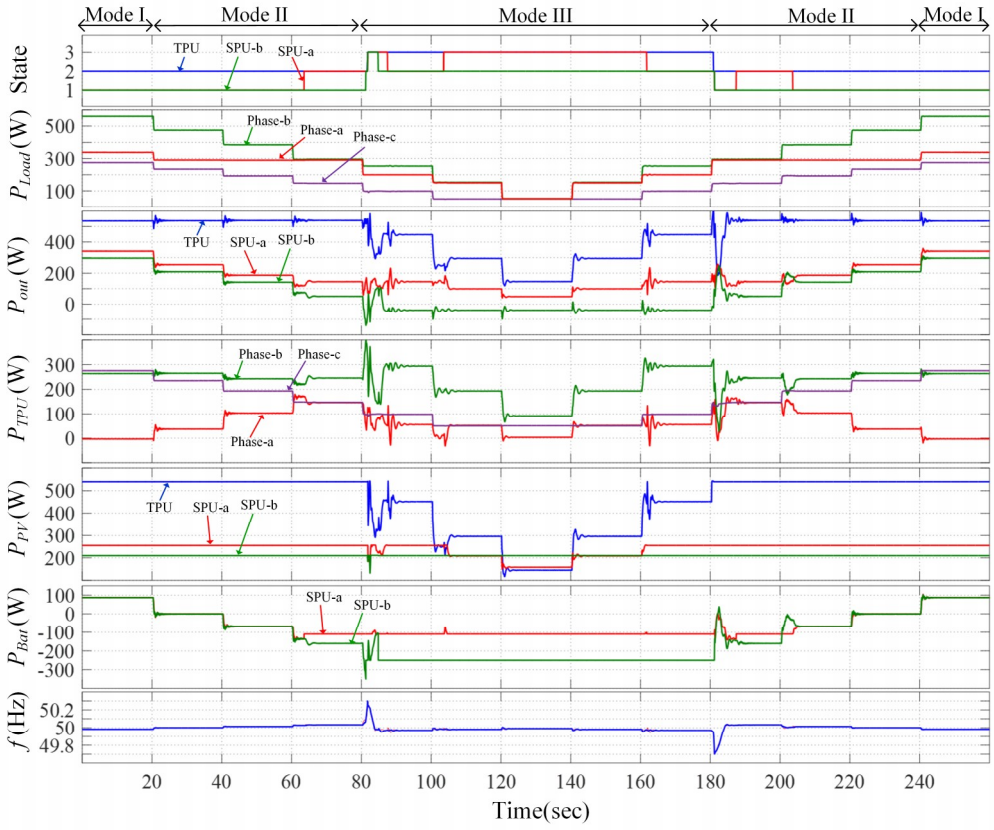

Fig. 6 Experimental results of a hybrid single/three-phase microgrid in different load conditions

in Mode I. The TPU is in State 2, the SPUs are in State 1, all PVs work at MPP and the remaining of the total load is shared between the SPUs according to (2) such that the battery discharging powers of them are equal, despite they are in different phases. The TPU controls power flow among the phases and $P_{TPU\text{-}a}$ is negative which means power is delivered from phase-a to other phases. At t=20s, the load is decreased to 1000W and total PV generation is higher than total load, therefore, the MG enters Mode II and the batteries are charged with equal powers determined by (5). At t=40s, the load is decreased to 870W and charging powers of batteries increase equally. At t=60s, the load is decreased to 735W. As a result, SPU-a that has the minimum $|P_{ChLimit}|$, reaches its maximum charging power and changes to State 2 with output power regulated to $P_{PV\text{-}MP}+P_{ChLimit}$. The SPU-b battery is charged with the remaining charging power. At t=80s, load is decreased to 550W. Consequently, SPU-b also reaches the maximum charging power and changes to State 2. Since all units are in State 2, frequency increases until saturates at f_{max}. At this point, all units change to State 3. However, since PV power is notsufficient for supplying both battery charging power and output power determined by (8) in SPU-a and SPU-b, they return to State 2. It is observed that the output power of SPU-b is negative. This implies that the unit absorbs power from the MG for charging its battery. At t=100s, the load is decreased to 355W. Since SPU-a and SPU-b are in State 2, regulated to a fixed output power, the output power of TPU decreases and f increases based on (8). After 3s, criterion (10) is validated in SPU-a and it returns to State 3. As a result, its PV generation drops accordingly. Note that according to m_p of TPU and

TABLE I
EXPERIMENTAL SETUP AND CONTROLLER PARAMETERS

Parameter	Symbol	Value	Unit
Nominal voltage	E^*	220	V_{rms}
Nominal frequency	f_0	50	Hz
Inverter rating	$P_{out\text{-}max}$	SPU:350 TPU:1050	W
Converter side inductance	L_f	3.6	mH
Filter capacitance	C	18	uF
Grid side inductance	L_o	3.6	mH
Virtual inductance	L_v	4	mH
Virtual resistance	R_v	1	Ω
Voltage loop PR	K_{pV}, K_{iV}	0.02, 15	-, S^{-1}
Current loop PR	K_{pI}, K_{iI}	10, 8000	-, S^{-1}
Voltage droop coefficient	m_q	0.007	V/Var
PCM PI controller	K_{PP}, K_{PI}	0.0016, 0.008	rad/(W.s), rad/(W.s^2)
Droop LPF bandwidth	ω_c	10	Hz
SoC balancing	m_{pd0}, m_{pc0}, n	0.000047, 0.064, 15	-

SPU- a in State 3, the output power of TPU is three times of SPU-a. At t=120s, the load is decreased to 150W and the output powers and consequently PV generations of TPU and SPU-a decrease, and SPU-b remains in State 2. At t=140s, the load is increased to 355W but there is no change in the State of the

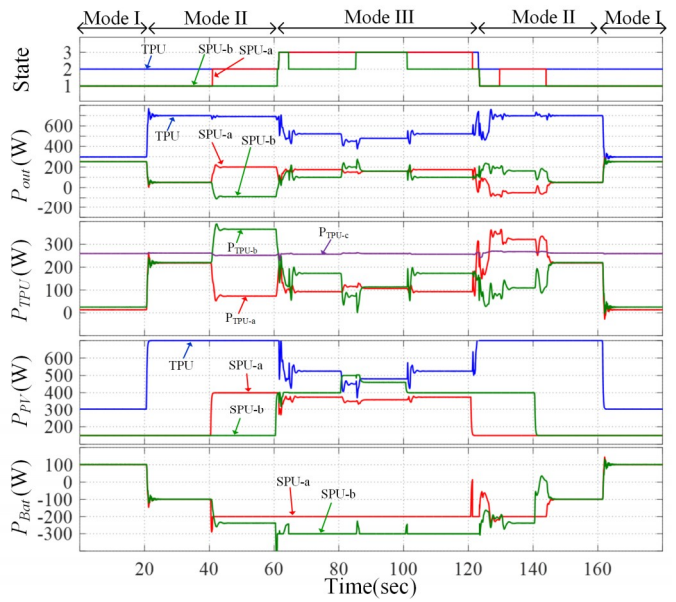

Fig. 7. Response of the system to $P_{PV\text{-}MP}$ variations while the load is constant

units. At t=160s, the load is increased to 550W and SPU-a reaches its maximum PV power and changes to State 2. At t=180s, the load is increased to 735W. Consequently, TPU also reaches its maximum PV power and changes to State 2. Since all units are in State 2, frequency decreases until saturates at f_{min}. At this point, SPU-a and SPU-b change to State 1 and the MG enters Mode II. However, since SPU-a battery charging power determined by (5) is more than its maximum value, it returns to State 2. At t=200s, the load is increased to 870W. Since TPU and SPU-a are in State 2 with constant output power, the output power of SPU-b increases, resulting in decrease in f based on (8). After 3s, SPU-a also changes to State 1 as the criterion (9) is validated. At this point, SPU-a and SPU-b are in State 1 having same battery charging powers. At t=220s, load is increased to 1000W and the charging powers of SPU-a and SPU-b decrease equally to -2W. At t=220s, load is increased to 1175W and the MG enters Mode I.

Fig. 7 shows the system response to $P_{PV\text{-}MP}$ variation of different units due to variation in irradiance while the load in each phase is kept constant (total load is 800W). Initially, $P_{PV\text{-}MP}$ of TPU, SPU-a and SPU-b are 300W, 150W and 150W, respectively. The MG is in Mode I and batteries have equal discharging power of 100W. At t=20s, the TPU $P_{PV\text{-}MP}$ is increased to 700W. Since total PV generation is more than load, the MG enters Mode II and the batteries have equal charging powers of 100W. At t=40s, the SPU-a $P_{PV\text{-}MP}$ is increased to 400W and it reaches the maximum charging power and changes to State 2. At t=60s, the SPU-b $P_{PV\text{-}MP}$ is increased to 400W and it also reaches the maximum charging power and changes to State 2. Since all units are in State 2, frequency increases until saturates at f_{max}. At this point, all units change to State 3 and the MG enters Mode III. However, PV power is not sufficient in SPU-b and it returns to State 2. At t=80s, the SPU-b $P_{PV\text{-}MP}$ is increased to 500W, criterion (10) is validated in SPU-b and it returns to State 3. At this point, all units are in State 3, SPUs have equal output power, one-third of TPU output power. At t=100s, the SPU-b $P_{PV\text{-}MP}$ is decreased to 400W, therefore it reaches its maximum PV power and changes to State 2.

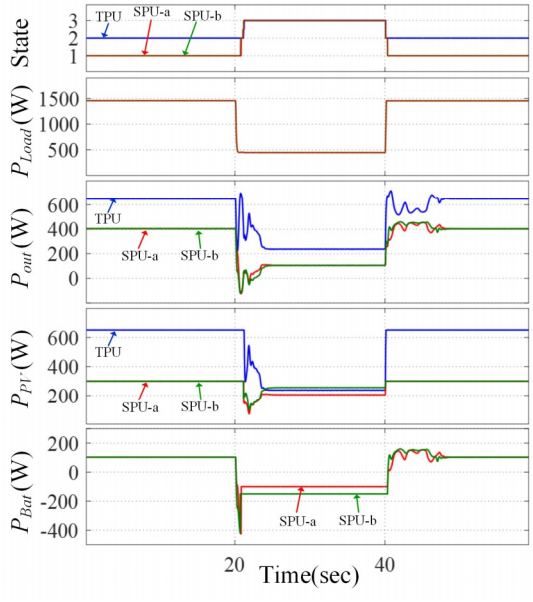

Fig. 8 Step load response

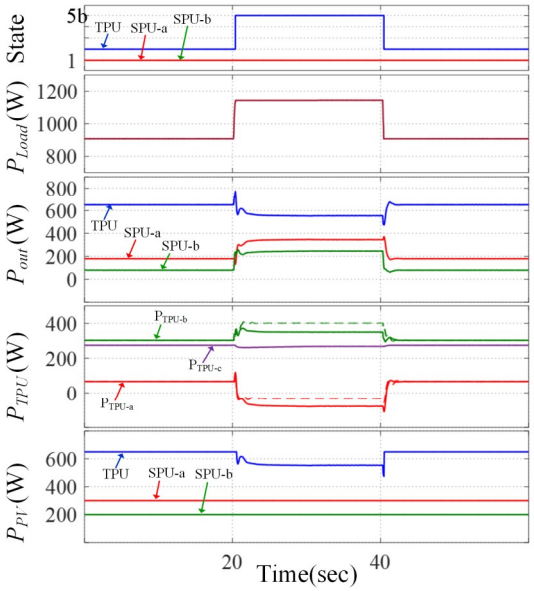

Fig. 9 Phase-b output power limiting in TPU

At t=120s, the SPU-a $P_{PV\text{-}MP}$ is decreased to 150W, therefore it also reaches its maximum PV power and changes to State 2. Since all units are in State 2, frequency decreases until saturates at f_{min}. At this point, SPU-a and SPU-b change to State 1 and the MG enters Mode II. But the battery charging power of SPU-a determined by (5) is more than its maximum value and it returns to State 2. At t=140s, the SPU-b $P_{PV\text{-}MP}$ is also decreased to 150W and the criterion (9) is validated and it returns to State 1. At t=160s, the TPU $P_{PV\text{-}MP}$ is decreased to 300W and the MG enters Mode I.

Fig. 8 shows the system response to step load change. At t=20s the load is changed from 1450W to 450 W and at t=40s it is returned to 1450W. The proposed method successfully changes the state of SPUs from State 1 and TPU from State 2 to State 3 and vice versa to cope with the load variations.

Fig. 9 shows phase power limiting in TPU. It is assumed that

the maximum power of each phase of the TPU is 350W. At

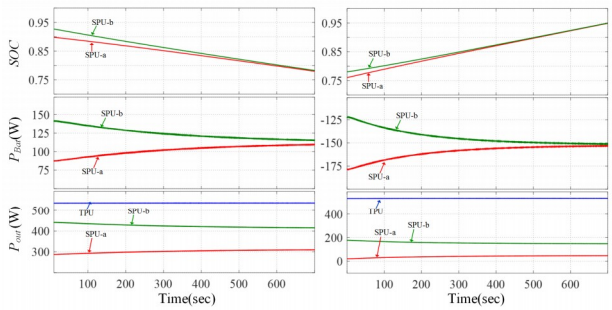

Fig. 10 SoC balancing in (left) discharging (Right) charging mode

t=20s, the load is increased from 900 to 1150W, as a result, phase-b output power of TPU reaches its limit and TPU changes to State 5b, with output power determined by (14). The output power and consequently, the PV power are decreased in order to limit the phase-b output power. The dashed lines in the P_{TPU} are the phase powers without power limiting. At *t*=40s the load is decreased to 900W and TPU returns to State 2.

Fig. 10 shows SoC balancing of the batteries in discharging and charging modes. The SPUs are in State 1 and the discharging power of the batteries are determined by (2) and (5) with n=15. In discharging mode, because of high imbalance between the SoCs, difference between battery discharging powers is high at start and SPU-b which has higher SoC, discharges with higher power. The SoCs, and consequently, battery discharging powers gradually converge. In charging mode, SPU-a that has lower SoC charges with higher power and finally the SoCs and battery charging powers converge.

II. Conclusion

In this paper, a decentralized control method is proposed for power management and load sharing in hybrid single/three-phase islanded MGs consisting of PV units, battery units and hybrid PV/battery units. The proposed method is not limited to single-phase and three-phase MGs or MGs with only separate PV and battery units. In this method, the whole MG can operate in three modes and according to load, PV generation and battery conditions, the operation of each unit in the MG is divided into five states for single-phase units and seven states for three-phase units, in which, frequency level is used as trigger for transition between the states. In each state, specific modified droop function is used for output power control and dc-link is regulated by one of PV boost converter, battery boost converter or regulating output power. Power flow among different phases is performed automatically through three-phase units, so that loads on a phase can be supplied from the generation in other phases, or batteries can be charged from the excess power of other phases. Several experimental results are performed to evaluate the performance of the proposed method in different possible conditions of a microgrid consisting of one three-phase unit and two single-phase units. The results show that the proposed method can successfully adopt the operating state, output power, PV generation and battery charging power of each unit to the MG operating conditions.

References

[1] J. M. Guerrero, M. Chandorkar, T. Lee, and P. C. Loh, "Advanced Control Architectures for Intelligent Microgrids; Part I: Decentralized and Hierarchical Control," *Industrial Electronics, IEEE Transactions on,* vol. 60, pp. 1254-1262, 2013.

[2] J. C. Vasquez, J. M. Guerrero, J. Miret, M. Castilla, V. de, x00F, *et al.*, "Hierarchical Control of Intelligent Microgrids," *Industrial Electronics Magazine, IEEE,* vol. 4, pp. 23-29, 2010.

[3] Z. Li, S. Kai, X. Yan, and X. Mu, "H6 Transformerless Full-Bridge PV Grid-Tied Inverters," *Power Electronics, IEEE Transactions on,* vol. 29, pp. 1229-1238, 2014.

[4] T. Kerekes, M. Liserre, R. Teodorescu, C. Klumpner, and M. Sumner, "Evaluation of Three-Phase Transformerless Photovoltaic Inverter Topologies," *Power Electronics, IEEE Transactions on,* vol. 24, pp. 2202-2211, 2009.

[5] H. Liu, P. C. Loh, X. Wang, Y. Yang, W. Wang, and D. Xu, "Droop Control with Improved Disturbance Adaption for PV System with Two Power Conversion Stages," *IEEE Transactions on Industrial Electronics,* vol. PP, pp. 1-1, 2016.

[6] I. Serban and C. Marinescu, "Control Strategy of Three-Phase Battery Energy Storage Systems for Frequency Support in Microgrids and with Uninterrupted Supply of Local Loads," *Power Electronics, IEEE Transactions on,* vol. 29, pp. 5010-5020, 2014.

[7] H. Fakham, L. Di, and B. Francois, "Power Control Design of a Battery Charger in a Hybrid Active PV Generator for Load-Following Applications," *Industrial Electronics, IEEE Transactions on,* vol. 58, pp. 85-94, 2011.

[8] J. M. Guerrero, J. C. Vasquez, J. Matas, M. Castilla, and L. G. de Vicuna, "Control Strategy for Flexible Microgrid Based on Parallel Line-Interactive UPS Systems," *Industrial Electronics, IEEE Transactions on,* vol. 56, pp. 726-736, 2009.

[9] H. Mahmood, D. Michaelson, and J. Jin, "Decentralized Power Management of a PV/Battery Hybrid Unit in a Droop-Controlled Islanded Microgrid," *Power Electronics, IEEE Transactions on,* vol. 30, pp. 7215-7229, 2015.

[10] M. Hamzeh, A. Ghazanfari, H. Mokhtari, and H. Karimi, "Integrating Hybrid Power Source Into an Islanded MV Microgrid Using CHB Multilevel Inverter Under Unbalanced and Nonlinear Load Conditions," *Energy Conversion, IEEE Transactions on,* vol. 28, pp. 643-651, 2013.

[11] C. Il-Yop, L. Wenxin, D. A. Cartes, E. G. Collins, Jr., and M. Seung-Il, "Control Methods of Inverter-Interfaced Distributed Generators in a Microgrid System," *Industry Applications, IEEE Transactions on,* vol. 46, pp. 1078-1088, 2010.

[12] H. Jinwei and L. Yun Wei, "An Enhanced Microgrid Load Demand Sharing Strategy," *Power Electronics, IEEE Transactions on,* vol. 27, pp. 3984-3995, 2012.

[13] B. Belvedere, M. Bianchi, A. Borghetti, C. A. Nucci, M. Paolone, and A. Peretto, "A Microcontroller-Based Power Management System for Standalone Microgrids With Hybrid Power Supply," *Sustainable Energy, IEEE Transactions on,* vol. 3, pp. 422-431, 2012.

[14] Y. K. Chen, Y. C. Wu, C. C. Song, and Y. S. Chen, "Design and Implementation of Energy Management System With Fuzzy Control for DC Microgrid Systems," *Power Electronics, IEEE Transactions on,* vol. 28, pp. 1563-1570, 2013.

[15] K. T. Tan, P. L. So, Y. C. Chu, and M. Z. Q. Chen, "Coordinated Control and Energy Management of Distributed Generation Inverters in a Microgrid," *Power Delivery, IEEE Transactions on,* vol. 28, pp. 704-713, 2013.

[16] K. T. Tan, X. Y. Peng, P. L. So, Y. C. Chu, and M. Z. Q. Chen, "Centralized Control for Parallel Operation of Distributed Generation Inverters in Microgrids," *Smart Grid, IEEE Transactions on,* vol. 3, pp. 1977-1987, 2012.

[17] K. Jong-Yul, J. Jin-Hong, K. Seul-Ki, C. Changhee, P. June Ho, K. Hak-Man, *et al.*, "Cooperative Control Strategy of Energy Storage System and Microsources for Stabilizing the Microgrid during Islanded Operation," *Power Electronics, IEEE Transactions on,* vol. 25, pp. 3037-3048, 2010.

[18] H. Kanchev, L. Di, F. Colas, V. Lazarov, and B. Francois, "Energy Management and Operational Planning of a Microgrid With a PV-Based Active Generator for Smart Grid Applications," *Industrial Electronics, IEEE Transactions on,* vol. 58, pp. 4583-4592, 2011.

[19] E. Serban and H. Serban, "A Control Strategy for a Distributed Power Generation Microgrid Application With Voltage- and Current-Controlled Source Converter," *Power Electronics, IEEE Transactions on,* vol. 25, pp. 2981-2992, 2010.

[20] W. Dan, T. Fen, T. Dragicevic, J. C. Vasquez, and J. M. Guerrero, "Autonomous Active Power Control for Islanded AC Microgrids With Photovoltaic Generation and Energy Storage System," *Energy Conversion, IEEE Transactions on,* vol. 29, pp. 882-892, 2014.

[21] J. G. de Matos, F. S.F.e Silva, and L. A. de S Ribeiro, "Power Control in AC Isolated Microgrids With Renewable Energy Sources and Energy Storage Systems," *Industrial Electronics, IEEE Transactions*

on, vol. 62, pp. 3490-3498, 2015.
[22] A. Urtasun, E. L. Barrios, P. Sanchis, and L. Marroyo, "Frequency-Based Energy-Management Strategy for Stand-Alone Systems With Distributed Battery Storage," *Power Electronics, IEEE Transactions on,* vol. 30, pp. 4794-4808, 2015.
[23] W. Dan, T. Fen, T. Dragicevic, J. C. Vasquez, and J. M. Guerrero, "A Control Architecture to Coordinate Renewable Energy Sources and Energy Storage Systems in Islanded Microgrids," *Smart Grid, IEEE Transactions on,* vol. 6, pp. 1156-1166, 2015.
[24] H. Mahmood, D. Michaelson, and J. Jin, "Strategies for Independent Deployment and Autonomous Control of PV and Battery Units in Islanded Microgrids," *Emerging and Selected Topics in Power Electronics, IEEE Journal of,* vol. 3, pp. 742-755, 2015.
[25] X. Sun, Y. Hao, Q. Wu, X. Guo, and B. Wang, "A Multifunctional and Wireless Droop Control for Distributed Energy Storage Units in Islanded AC Microgrid Applications," *IEEE Transactions on Power Electronics,* vol. PP, pp. 1-1, 2016.
[26] X. Tang, X. Hu, N. Li, W. Deng, and G. Zhang, "A Novel Frequency and Voltage Control Method for Islanded Microgrid Based on Multienergy Storages," *IEEE Transactions on Smart Grid,* vol. 7, pp. 410-419, 2016.
[27] K. De Brabandere, B. Bolsens, J. Van den Keybus, A. Woyte, J. Driesen, R. Belmans*, et al.*, "A voltage and frequency droop control method for parallel inverters," in *Power Electronics Specialists Conference, 2004. PESC 04. 2004 IEEE 35th Annual*, 2004, pp. 2501-2507 Vol.4.
[28] J. M. Guerrero, J. C. Vasquez, J. Matas, V. de, x00F, L. G. a*, et al.*, "Hierarchical Control of Droop-Controlled AC and DC Microgrids;A General Approach Toward Standardization," *Industrial Electronics, IEEE Transactions on,* vol. 58, pp. 158-172, 2011.
[29] Q. Shafiee, J. M. Guerrero, and J. C. Vasquez, "Distributed Secondary Control for Islanded Microgrids;A Novel Approach," *Power Electronics, IEEE Transactions on,* vol. 29, pp. 1018-1031, 2014.
[30] Y. Karimi, H. Oraee, M. Golsorkhi, and J. Guerrero, "Decentralized Method for Load Sharing and Power Management in a PV/Battery Hybrid Source Islanded Microgrid," *IEEE Transactions on Power Electronics,* vol. PP, pp. 1-1, 2016.
[31] S. Qiuye, Z. Jianguo, J. M. Guerrero, and Z. Huaguang, "Hybrid Three-Phase/Single-Phase Microgrid Architecture With Power Management Capabilities," *Power Electronics, IEEE Transactions on,* vol. 30, pp. 5964-5977, 2015.
[32] J. C. Vasquez, J. M. Guerrero, M. Savaghebi, J. Eloy-Garcia, and R. Teodorescu, "Modeling, Analysis, and Design of Stationary-Reference-Frame Droop-Controlled Parallel Three-Phase Voltage Source Inverters," *Industrial Electronics, IEEE Transactions on,* vol. 60, pp. 1271-1280, 2013.
[33] J. M. Guerrero, H. Lijun, and J. Uceda, "Control of Distributed Uninterruptible Power Supply Systems," *Industrial Electronics, IEEE Transactions on,* vol. 55, pp. 2845-2859, 2008.
[34] J. M. Guerrero, L. Garcia De Vicuna, J. Matas, M. Castilla, and J. Miret, "Output Impedance Design of Parallel-Connected UPS Inverters With Wireless Load-Sharing Control," *Industrial Electronics, IEEE Transactions on,* vol. 52, pp. 1126-1135, 2005.
[35] H. Jinwei, L. Yun Wei, J. M. Guerrero, F. Blaabjerg, and J. C. Vasquez, "An Islanding Microgrid Power Sharing Approach Using Enhanced Virtual Impedance Control Scheme," *Power Electronics, IEEE Transactions on,* vol. 28, pp. 5272-5282, 2013.
[36] J. Matas, M. Castilla, V. de, x00F, L. G. a, J. Miret*, et al.*, "Virtual Impedance Loop for Droop-Controlled Single-Phase Parallel Inverters Using a Second-Order General-Integrator Scheme," *Power Electronics, IEEE Transactions on,* vol. 25, pp. 2993-3002, 2010.
[37] L. Xiaonan, S. Kai, J. M. Guerrero, J. C. Vasquez, and H. Lipei, "State-of-Charge Balance Using Adaptive Droop Control for Distributed Energy Storage Systems in DC Microgrid Applications," *Industrial Electronics, IEEE Transactions on,* vol. 61, pp. 2804-2815, 2014.
[38] L. Xiaonan, S. Kai, J. M. Guerrero, J. C. Vasquez, and H. Lipei, "Double-Quadrant State-of-Charge-Based Droop Control Method for Distributed Energy Storage Systems in Autonomous DC Microgrids," *Smart Grid, IEEE Transactions on,* vol. 6, pp. 147-157, 2015.

Yaser Karimi received the B.S and M.S. degrees in electrical engineering from Sharif University of Technology, Tehran, Iran, in 2008 and 2010, respectively, where he is currently working toward the Ph.D. degree. In 2015, he was a Visiting PhD Student with the Department of Energy Technology, Aalborg University, Aalborg, Denmark. His research interests include power electronics, power converters for renewable energy systems and microgrids.

Hashem Oraee (SM'95) graduated with a First Class Honors degree in Electrical and Electronics Engineering from University of Wales in Cardiff, UK in 1980 and a PhD in Electrical Machines from University of Cambridge, UK in 1984. He is currently a Professor of Electrical Engineering at Sharif University in Iran and the President of Iran Wind Energy Association. His research interests include various aspects of electrical machines, renewable energy and energy economics. He is Fellow of IET and a Senior Member of IEEE.

Josep M. Guerrero (S'01-M'04-SM'08-FM'15) received the B.S. degree in telecommunications engineering, the M.S. degree in electronics engineering, and the Ph.D. degree in power electronics, all from the Technical University of Catalonia, Barcelona, Spain, in 1997, 2000, and 2003, respectively.
He was an Associate Professor with the Department of Automatic Control Systems and Computer Engineering, Technical University of Catalonia, Barcelona, Spain. Since 2011, he has been a Full Professor with the Department of Energy Technology, Aalborg University, Aalborg, Denmark, where he is responsible for the microgrid research program. Since 2012, he has also been a Guest Professor with the Chinese Academy of Science and the Nanjing University of Aeronautics and Astronautics.